Efficiency improvement and image quality of organic light-emitting display by attaching cylindrical microlens arrays

Jiun-Haw Lee[1], Yu-Hsuan Ho[1], Kuan-Yu Chen[1], Hoang-Yan Lin[1], Jheng-Hao Fang[2], Sheng-Chih Hsu[1], Jia-Rong Lin[2], and Mao-Kuo Wei[2]*

[1] Graduate Institute of Photonics and Optoelectronics and Department of Electrical Engineering, National Taiwan University, Taipei, Taiwan 106, Republic of China

[2] Institute of Opto-Electronic Engineering and Department of Materials Science and Engineering, National Dong Hwa University, Hualien, Taiwan 974, Republic of China

mkwei@mail.ndhu.edu.tw

Abstract: In this paper, cylindrical microlens arrays with two different alignments were proposed to be applied in a commercial mobile phone having an organic light-emitting diode (OLED) panel. It was found that the parallel-aligned cylindrical array had better performance than the vertical-aligned one for the OLED panel. The parallel-aligned cylindrical microlens array can increase the luminous current efficiency at surface normal and the luminous power efficiency of the OLED panel by 45% and 38%, respectively. Besides, it can also make the spectrum of the OLED panel more insensitive to the viewing angle. Though it can slightly blur the image on the OLED panel, the universal image quality index can be maintained at a level of 0.8630.

OCIS codes: (080.3630) Lenses; (120.2040) Display; (110.3000) Image quality assessment.

Reference and links

1. C. W. Tang and S. A. Vanslyke, "Organic electroluminescent diodes," Appl. Phys. Lett. **51**, 913-915 (1987)
2. M.-H. Lu and J. C. Sturm, "Optimization of external coupling and light emission in organic light-emitting devices: modeling and experiment," J. Appl. Phys. **91**, 595-604 (2002)
3. Y. R. Do, Y.-C. Kim, Y.-W. Song, and Y.-H. Lee, "Enhanced light extraction efficiency from organic light emitting diodes by insertion of a two-dimensional photonic crystal structure," J. Appl. Phys. **96** 7629-7636 (2004)
4. T. Yamasaki, K. Suminoka, and T. Tsutsui, "Organic light-emitting devices with an ordered monolayer of silica microspheres as a scattering medium," Appl. Phys. Lett. **76** 1243-1245 (2000)
5. H.-Y. Lin, J.-H. Lee, M.-K. Wei, C.-L. Dai, C.-F. Wu, Y.-H. Ho, H.-Y. Lin, and T.-C. Wu, "Improvement of the outcoupling efficiency of an organic light-emitting device by attaching microstructured films," Opt. Commun. **275**, 464-469 (2007)
6. L. Lin, T. K. Shia, and C.-J. Chiu, "Silicon-processed plastic micropyramids for brightness enhancement applications," J. Micromech. Microeng. **10** 395-400 (2000)
7. S. Möller and S. R. Forrest, "Improved light out-coupling in organic light-emitting diodes employing ordered microlens arrays," J. Appl. Phys. **91**, 3324-3327 (2002)
8. M.-K. Wei and I-L. Su, "Method to evaluate the enhancement of luminance efficiency in planar OLED light emitting devices for microlens array," Opt. Express **12**, 5777-5782 (2004)
9. H. Peng, Y. L. Ho, X.-J. Yu, M. Wong, and H.-S. Kwok, "Coupling efficiency enhancement in organic light-emitting devices using microlens array-theory and experiment," J. Display Technol. **1**, 278-282 (2005)
10. Y. Sun and S. R. Forrest, "Organic light emitting devices with enhanced outcoupling via microlenses fabricated by imprint lithography," J. Appl. Phys. **100**, 073106 (2006)
11. M.-K. Wei, I-L. Su, Y.-J. Chen, M. Chang, H.-Y. Ling, and T.-C. Wu, "The influence of a microlens array on planar organic light-emitting devices," J. Micromech. Microeng. **16**, 368-374 (2006)
12. M.-K. Wei, J.-H. Lee, H.-Y. Lin, Y.-H. Ho, K.-Y. Chen, C.-C. Lin, C.-F. Wu, H.-Y. Lin, J.-H. Tsai, and T.-C. Wu, "Efficiency improvement and spectral shift of an organic light-emitting device by attaching a hexagon-based microlens array," J. Opt. A: Pure Appl. Opt. **10**, 055302 (2008)
13. H.-Y. Lin, Y.-H. Ho, J.-H. Lee, K.-Y. Chen, J.-H. Fang, S.-C. Hsu, M.-K. Wei, H.-Y. Lin, J.-H. Tsai, and T.-C. Wu, "Patterned microlens array for efficiency improvement of small-pixelated organic light-emitting

#101746 - $15.00 USD Received 18 Sep 2008; revised 15 Nov 2008; accepted 4 Dec 2008; published 8 Dec 2008

devices," Opt. Express **16**, 11044-11051 (2008)
14. Z. Wang and A. C. Bovik, "A universal image quality index," IEEE Signal Process. Lett. **9**, 81-84 (2002)

1. Introduction

In recent years, organic light-emitting displays (OLEDs) have been successfully applied to the small- and medium-sized displays of mobile electronics. Large-sized OLED televisions have also been demonstrated. Due to self emission, fast response time, and potentially low cost, the OLED is one of the most promising candidates for the next-generation displays [1]. However, due to waveguiding phenomena in the anode/organic layers and the substrate, the outcoupling efficiency of the bottom-emitting OLED is limited to less than 30% [2]. To increase the outcoupling efficiency of the OLED, many microstructures, such as photonic crystals, silica microspheres, micro-V-grooves, micropyramids, and microlenses, have been used to extract light rays trapped in the substrate and the anode/organic layers [3-13]. Since the spectrum of the OLED with photonic crystals and microspheres varies strongly at different viewing angles, they are not suitable to be applied in displays [3,4]. For micro-V-grooves and micropyramids, they can improve less efficiency and have more spectral shifts of the OLED than microlenses [5,6,12]. Therefore, microlenses are one of the best means to increase efficiency of the OLED.

As reported by Möller and Forrest [7] and Peng et al. [9], though spherical microlenses can improve luminous power efficiency up to 85%, they did result in the image blurring of the OLEDs. We also tried to attach a regular spherical microlens array, having a diameter and a gap of 10 and 2.5 μm respectively, on an active-matrix full-color OLED panel and observed the variation of image quality of a single blue subpixel before and after the attachment, as shown in Fig. 1. Without microlenses, the blue OLED subpixel showed a clear rectangular image, as depicted in Fig. 1(a). This image was formed due to the emitting light rays having incident angles at glass/air interface less than the critical angle (~41.8°). However, this blue subpixel possessed a blurring image, which was larger than twice of the original image without microlenses (Fig. 1(b), when attached with the spherical microlenses (Fig. 1(c)). This image blurring came from microlenses outside the emitting region of the blue subpixel, since microlenses changed incident angles of emitting light rays at glass/air interface, as described in Ref. 13. Thus, spherical microlens arrays seem to be suitable only for the OLED lighting applications.

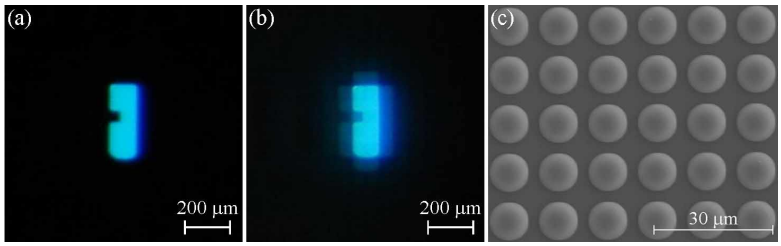

Fig. 1. The photographs of a blue OLED subpixel: (a) without any microstructures and (b) with a regular microlens array attachment. (c) The microphotograph of the regular spherical microlens array.

Although regular spherical microlens arrays may not be possibly used in displays, are the other shapes and arrangements of microlenses not fitting in these applications? This is the purpose of this study to propose a regular cylindrical microlens array with different alignments in the OLED displays. The efficiency improvement and image quality of the OLED panel attached with cylindrical microlens arrays will be focused on.

2. Experimental methods

The fabrication process of cylindrical microlens arrays is illustrated in Fig. 2, which is very similar to that reported in Ref. [13], except the shapes of photoresist patterns. First, a (100)

#101746 - $15.00 USD Received 18 Sep 2008; revised 15 Nov 2008; accepted 4 Dec 2008; published 8 Dec 2008

silicon wafer was used as a substrate. Second, the photoresist AZ P4620 was spun on the wafer. Third, photoresist strips were made through photolithographic process. The length, width, and gap distance of these strips were set at 20, 10, and 2.5 μm, respectively. Fourth, these strips were heated at 230°C for 44 hrs to transform themselves into the shape of cylindrical caps. Fifth, liquid polydimethylsiloxane (PDMS) mixed with its hardener was poured onto the wafer and put in an oven to be thermally cured at 65°C for 4 hrs. Sixth, the hardened PDMS mold with a concave cylindrical microlens array on the mold surface was then released by peeling off the mold from the wafer. Seventh, liquid UV-curable PMMA was coated between the PDMS mold and PET film, followed by UV exposure at 1 J/cm^2 to harden the PMMA. Finally, a flexible PET film with the duplicated cylindrical microlens array on the film surface was formed after separating the film from the mold.

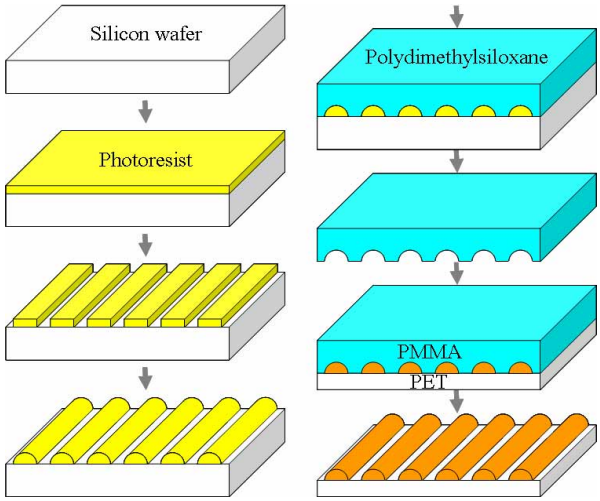

Fig. 2. The fabrication process of cylindrical microlens arrays.

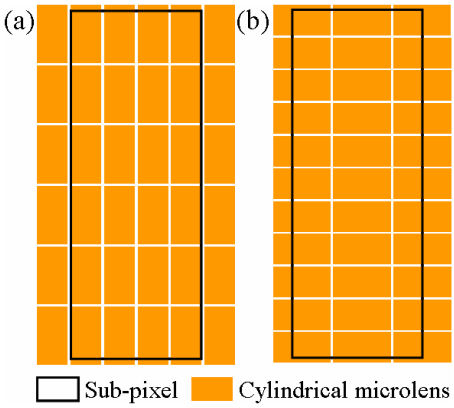

Fig. 3. Schematic alignments of cylindrical microlens arrays: (a) parallel and (b) vertical.

In this study, an active-matrix full-color OLED panel of a mobile phone (BenQ Siemens, S88) was selected. Before the usage, a circular polarizer film on the panel surface was removed. Images on the panel were then loaded from a personal computer, and the brightness of each subpixel (blue, green, and red) can also be adjusted. To study the influence of cylindrical microlens array on the image quality and efficiency improvement of the OLED panel, it was attached on the panel by using refractive-index-matched silicone oil into two different arrangements, as shown in Fig. 3. For the parallel alignment, the longer edges of microlenses were parallel to the longer edges of subpixels, while being perpendicular to the

#101746 - $15.00 USD Received 18 Sep 2008; revised 15 Nov 2008; accepted 4 Dec 2008; published 8 Dec 2008

longer edges of subpixels for the vertical alignment.

The length and width of base region, the gap distance, and the sag of cylindrical microlenses was measured with a scanning electron microscope (Hitachi S3500). A spectroradiometer (Minolta CS-1000A) was used to measure the luminance and spectrum of the device in dark environment to minimize the influence of ambient light. For the angular-dependent luminance measurement, the device was fixed on a rotational stage, and the luminance was then measured at different viewing angles from 0° to 70°.

The images on the OLED panel attached with and without cylindrical microlenses were recorded by using a digital camera. The format of photos was then changed from RGB mode to gray-level mode for the calculation of image quality.

3. Results and discussion

Typical cylindrical microlens array on the PET film was depicted in Fig. 4. The length and width of baser region of cylindrical microlenses were 20 and 10 μm, respectively. The gap distance between adjacent microlenses was 2.5 μm.

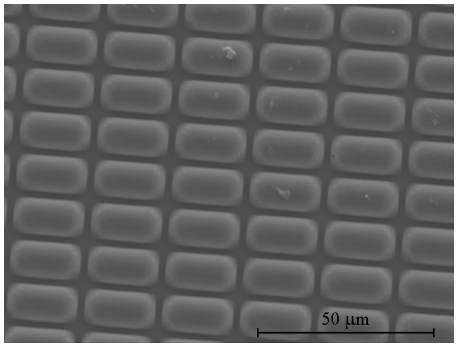

Fig. 4. Microphotograph of cylindrical microlenses.

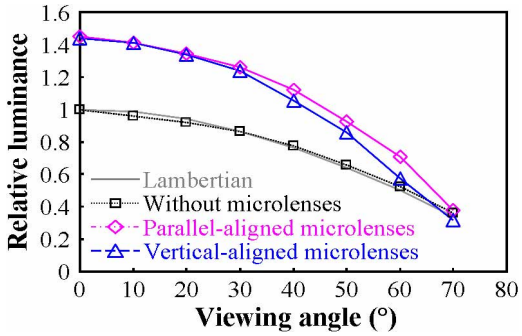

Fig. 5. The angular-dependent luminance of the OLED panel attached with and without cylindrical microlenses.

When all the blue subpixels in the panel without microlenses were driven, its luminance decreased with increasing the viewing angle, as shown in Fig. 5. This angular-dependent luminance reveals that the panel is a Lambertian-like light source. As the cylindrical microlens arrays were attached in turn on the same panel, the device luminance also decreased with increasing the viewing angles. Since the ratio of the luminous current efficiencies of the panel with microlenses to that without microlenses is equal to the ratio of their luminance [12], the luminous current efficiency perpendicular to the panel is increased 45% and 44% when attached with parallel- and vertical-aligned cylindrical microlens arrays, respectively. It is also to note that the ratio of the luminous power efficiencies of the panel with microlenses to that of the panel without microlenses equals the ratio of their luminous exitances [12]. Thus, the luminous power efficiency of the panel was improved 38% and 27% when attached with

#101746 - $15.00 USD Received 18 Sep 2008; revised 15 Nov 2008; accepted 4 Dec 2008; published 8 Dec 2008

parallel- and vertical-aligned cylindrical microlens arrays, respectively.

Figure 6 shows the spectra of the OLED panel (only blue subpixels were lighting on) attached with and without the cylindrical and spherical microlens arrays at different viewing angles. As observed from the experimental data, the angular-dependent spectra of the panel attached with either vertical-aligned cylindrical or spherical microlenses were very similar to the OLED panel attached with the parallel-aligned cylindrical ones. In Fig. 6, two peaks (at ~468 and ~499 nm) and one shoulder (at ~540 nm) existed in all the spectra of the device regardless of both the attached microlenses and .the viewing angles. Besides, the relative intensities of both the peak at 499 nm and the shoulder at 540 nm increased with increasing the viewing angle. This meant that more light rays with longer wavelengths were extracted at the larger viewing angles. Therefore, there were red shifted for increasing the viewing angle. However, the spectra of the panel, especially at the 499-nm peak and 540-nm shoulder, had less variation in the studied range of the viewing angle when attached with either cylindrical or spherical microlenses than without. This meant that the spectra of the panel attached with either cylindrical or spherical microlenses are more insensitive to the viewing angle than that without microlenses.

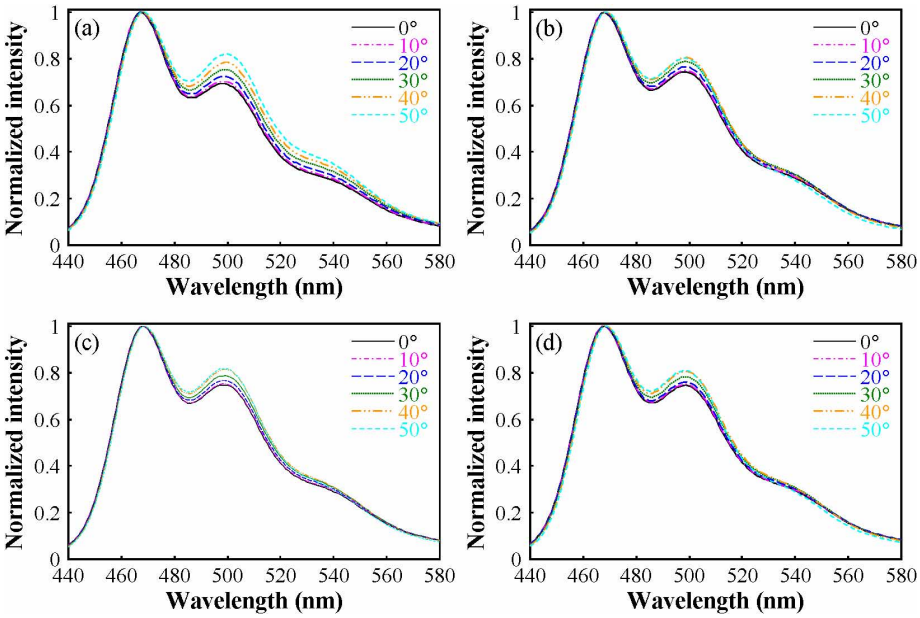

Fig. 6. (a). The angular-dependent spectra of the OLED panel without microlenses. The spectra of the OLED panel attached with a (a) parallel- and (c) vertical-aligned cylindrical, and (d) spherical microlens array at different viewing angles.

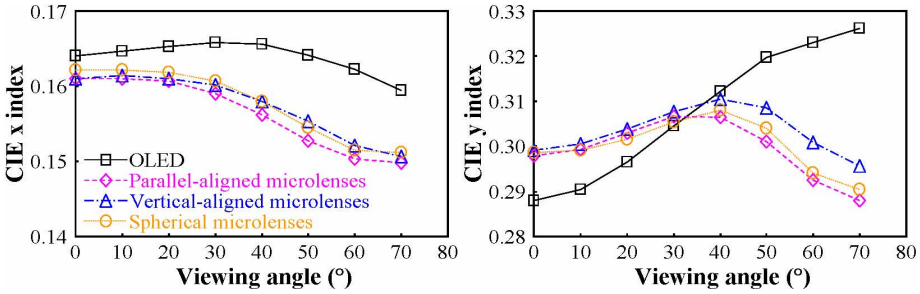

Fig. 7. The CIE coordinates of the OLED panel attached with/without a cylindrical or spherical microlens array at different viewing angles.

#101746 - $15.00 USD Received 18 Sep 2008; revised 15 Nov 2008; accepted 4 Dec 2008; published 8 Dec 2008

The CIE coordinates of the OLED panel attached with and without either cylindrical or spherical microlenses at different viewing angles were depicted in Fig. 7. For the panel without microlenses, the CIE x index increased first and then decreased, and the CIE y index monolithically increased with increasing the viewing angle. The maximal variations of the CIE x and CIE y indices of the panel were 0.006 and 0.038, respectively, in the studied range of the viewing angle. When the panel attached with either cylindrical or spherical microlenses, however, the CIE x index decreased, and the CIE y index increased initially and then decreased with increasing the viewing angle. The maximal variations of the CIE x and CIE y indices were 0.011 and 0.015-0.019, respectively, in the studied viewing angles, as illustrated in Table 1. Comparing the variation of the CIE coordinates, the panel without microlenses has slightly smaller variation in the CIE x index and much larger variation in the CIE y index at the studied viewing angles than that with microlenses. Therefore, the panel attached with either cylindrical or spherical microlenses is more insensitive to the viewing angle than the panel without microlenses.

Table 1. The maximal variation of CIE indices of the OLED panel attached with and without cylindrical and spherical microlens arrays at the studied range of the viewing angle.

Items	Without microlenses	Parallel-aligned cylindrical microlenses	Vertical-aligned cylindrical microlenses	Spherical microlenses
$(CIE\ x)_{max} - (CIE\ x)_{min}$	0.006	0.011	0.011	0.011
$(CIE\ y)_{max} - (CIE\ y)_{min}$	0.038	0.019	0.015	0.018

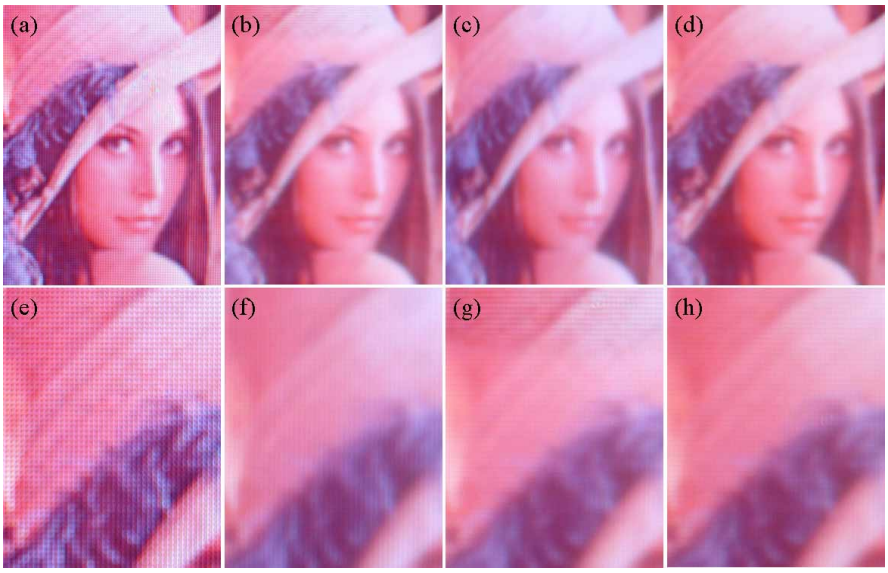

Fig. 8. (a) The original Lena image on the OLED panel. (b) The Lena images on the panel attached with (b) parallel- and (c) vertical-aligned cylindrical and (d) spherical microlens arrays, respectively. (e), (f), (g) and (h) are the magnified pictures on the upper parts of (a), (b), (c) and (d), respectively.

Figure 8(a) shows a clear Lena image loaded on the panel without microlenses. When the parallel-, vertical-aligned cylindrical and spherical microlens arrays were attached in turn on the panel, their Lena images became bright and reddish, as described in Figs. 7(b)-7(d), respectively. The variation of Lena images can be explained by the efficiency improvement and the red shift of spectra, as shown in Figs. 5 and 6, when the panel attached with cylindrical and spherical microlens arrays. It can also be observed that the resolutions of the

#101746 - $15.00 USD Received 18 Sep 2008; revised 15 Nov 2008; accepted 4 Dec 2008; published 8 Dec 2008

Lena images were the best and the worse when the panel attached with a parallel-aligned cylindrical and a spherical microlens array, respectively, as shown in Figs. 7(f)-7(h).

To judge the quality of the Lena image displayed on the panel, a universal image quality index (Q) was introduced [14]. Supposed that $x = \{x_i \mid i = 1, 2, \ldots, N\}$ and $y = \{y_i \mid i = 1, 2, \ldots, N\}$ are the gray scale values of each pixels of the original and test image signals, respectively. N is the total pixel number. The universal image quality index (Q) is defined as

$$Q = \frac{\sigma_{xy}}{\sigma_x \sigma_y} \cdot \frac{2\bar{x}\bar{y}}{\bar{x}^2 + \bar{y}^2} \cdot \frac{2\sigma_x \sigma_y}{\sigma_x^2 + \sigma_y^2} \tag{1}$$

where $\bar{x}$ and $\bar{y}$ are the average values, σ_x and σ_y are the standard deviations, and σ_{xy} is the covariance of x and y, respectively. Thus, the universal image quality index comprises three components: the correlation coefficient, the mean luminance difference, and the contrast similarity between the original and test images.

Table 2 shows the calculation results, based on Eq. (1), of the three parameters and the universal image quality index of the panel attached with cylindrical and spherical microlens arrays. Since the universal image quality index of the panel attached with a parallel-aligned cylindrical microlens array (0.8630) was larger than that attached with the other two microlens arrays, the panel attached with parallel-aligned microlenses had better image quality. The better performance in the parallel-aligned case came from the larger correlation coefficient and contrast similarity.

Table 2. Quantities of each term and overall image quality indices of the panel attached with cylindrical microlens arrays.

Items	Correlation coefficient	Mean luminance difference	Contrast similarity	Universal image quality index
Parallel-aligned microlenses	0.9003	0.9994	0.9567	0.8630
Vertical-aligned microlenses	0.8661	0.9992	0.9448	0.8213
Regular spherical microlenses	0.8435	0.9969	0.9414	0.7933

4. Conclusions

It was found that both the parallel- and vertical-aligned cylindrical microlens arrays can efficiently improve both the luminous current efficiency at surface normal and the luminous power efficiency of the OLED panel. The spectra were more insensitive to the viewing angle when the panel was attached with either the parallel- or vertical-aligned cylindrical microlens arrays. Besides, these two cylindrical microlens arrays did not severely blur the image of the panel. Comparing to the vertical-aligned cylindrical microlens array, the parallel-aligned one can not only enhance more the luminous current efficiency and luminous power efficiency but also have better image quality of the panel. Therefore, the parallel-aligned cylindrical microlens array seems to be a good choice for the OLED displays, especially for the large-sized.

Acknowledgments

The authors gratefully acknowledge the financial support given by the National Science Council of the Republic of China under projects NSC 97-2221-E-002-056, NSC 97-2221-E-259-009, and NSC 96-2221-002-118. We also acknowledge the financial support by Chung-Shan Institute of Science and Technology of the Republic of China.

#101746 - $15.00 USD Received 18 Sep 2008; revised 15 Nov 2008; accepted 4 Dec 2008; published 8 Dec 2008